Novel Cell Nucleus Directed Fluorescent Tetraazacyclododecane-Tetraacetic Acid Compounds

A. Sturzu[1,2], U. Klose[1], H. Echner[2], M. Regenbogen[1], H. Kalbacher[2], A. Gharabaghi[3] and S. Heckl[1,*]

[1]*Department of Neuroradiology, University of Tübingen,* [2]*Peptide synthesis laboratory, Interfaculty Institute of Biochemistry, University of Tübingen,* [3]*Department of Neurosurgery, University of Tübingen*

Abstract: Peptide conjugates derived from the SV 40 T antigen nuclear localisation sequence (NLS) have been successfully used to translocate both fluorescein isothiocyanate (FITC) and Gadolinium (Gd)-1,4,7,10-tetraazacyclododecane-1,4,7,10-tetraacetic acid (DOTA) into the cytoplasm and nucleus of glioma cells. However, uptake occurred only in up to 35% of cells.

To improve cellular uptake, we designed three novel FITC-labelled Gd-DOTA conjugates.

In the first conjugate, the commonly used Gd-DOTA-complex was coupled to the nuclear localization sequence (NLS) of the Simian Virus (SV) 40 T antigen alone as a control. In the second conjugate, the Gd-DOTA-coupled SV 40 T antigen NLS was elongated by the HIV-1 tat peptide (HIV-NLS).

A third conjugate, in which the Gd-DOTA-complex was coupled to the SV 40 T antigen NLS elongated by a peptide containing seven arginines and six aminohexanoic acids (Ahx6R7) was also synthesized (AHX-NLS).

By means of confocal laser scanning microscopy, fluorescence activated cell sorting, magnetic resonance imaging (MRI) and viability tests we were able to demonstrate that the first conjugate containing only the NLS of the SV 40 T antigen stained the nuclei of no more than 10-12% of U373 and LN18 glioma cells, resulting in low signal intensity in MRI. The stained cells remained viable. After incubation with conjugates HIV-NLS and AHX-NLS the nuclei of up to 73% of U373 and LN18 glioma cells were stained. This was associated with high signal intensity in MRI and cell death.

As previously shown, the gadolinium ion reduces cellular uptake of DOTA conjugates. To confirm this, the conjugates were produced with or without gadolinium.

The gadolinium-free DOTA conjugates showed a higher cellular uptake rate and an increased cytotoxic potential.

Key Words: HIV-1 tat, aminohexanoic acid, tetraazacyclododecane-tetraacetic acid, gadolinium, cellular uptake, NLS.

1. INTRODUCTION

The gadolinium (Gd) 1,4,7,10-tetraazacyclododecane-1, 4,7,10-tetraacetic acid (DOTA) complex (0.56 kDa, 0.9 nm diameter [1]) is commonly used as an extracellular contrast agent in magnetic resonance imaging (MRI) and is not taken up by the cytoplasm and the cell nucleus [2].

The nuclear localisation sequence (NLS, PKKKRKV) of the SV 40 T antigen has been shown to transport proteins from the cytoplasm into the cell nucleus [3].

Gd-DOTA was coupled to the SV 40 T antigen NLS elongated by four arginines (PKKKRKVRRRRK(FITC)GGK(DOTA). Only up to 35% of glioma cells showed uptake of the correct as well as a mutant NLS-DOTA conjugate [4].

The present work represents a continuation of these previous investigations [4].

*Address correspondence to this author at the Department of Neuroradiology, University of Tübingen, Hoppe-Seyler-Str.3, 72076 Tübingen, Germany; Tel: 0049 7071-2986024; E-mail: stefan.heckl@med.uni-tuebingen.de

We tried to optimize the cellular uptake of NLS-DOTA conjugates by using different peptide sequences containing more cationic amino acids than the original four arginines. Additionally the NLS-DOTA conjugate without the four arginines was used as a further control.

Three DOTA peptide conjugates were used:

1. the NLS of the SV 40 T antigen alone (abbreviated: **NLS**):

PKKKRKV-K(FITC)GGK(DOTA)

2. the NLS of the SV 40 T antigen elongated by the basic domain Tat_{49-57} of HIV-1 (abbreviated: **HIV-NLS**, [5,6]):

PKKKRKV*RKKRRQRRR*-K(FITC)GGK(DOTA)

3. the NLS of the SV 40 T antigen elongated by a novel peptide containing 6 aminohexanoic acids (X) and 7 arginines (R) (abbreviated: **AHX-NLS**):

PKKKRKV*RXRXRXRXRXRXR*-K(FITC)GGK(DOTA)

Aminohexanoic acids were incorporated to reduce the allergenic potential of the conjugate in future animal studies

1573-4064/09 $55.00+.00

(polyarginines may induce microvascular leakage of macromolecules [7]).

To enable confirmation of the nuclear localization by live cell confocal laser scanning microscopy the conjugates were linked to fluorescein isothiocyanate (FITC).

In addition to the Gd-free DOTA conjugates, the same conjugates were also produced with Gd-DOTA (abbreviated: **Gd-NLS**, **Gd-HIV-NLS**, **Gd-AHX-NLS**).

2. MATERIALS AND METHODS

2.1. Synthesis of Conjugates

Synthesis was performed by solid phase peptide synthesis on an Eppendorf ECOSYN P peptide synthesizer (Eppendorf-Biotronik, Hamburg, Germany) employing the fmoc strategy. The amino group was protected with fmoc (9-fluorenylmethyloxycarbonyl) which can be cleaved off under alkaline conditions. Tentagel S rink amid resin (Rapp-Polymere, Tübingen, Germany) was used as carrier material. Synthesis was carried out on a scale of 0.1 mmol. Four time excess of fmoc-protected amino acids were coupled to the resin in a 40 minute reaction using 4 equivalents of TBTU [2-(1H-benzotriazole-1-yl)-1,1,3,4-tetramethyluronium tetrafluoroborate] as coupling reagent and 8 equivalents of DIPEA (diisopropylethylamine) as an adjuvant base. Amino acid side chains were protected by following protective groups: Lysine: tert.-butyl-oxycarbonyle (tBoc), Arginine: (Pbf) N^6-2,2,4,6,7-pentamethyl-dihydrobenzofurane-5-sulfo-nyl.

Lysine side chains designated for DOTA were protected with Mmt (4-methoxytrityl). Lysine side chains carrying a fluorescein urea derivate were protected with Dde (1-(4,4-dimethyl-2,6-dioxocyclohex-1-ylidene)-ethyl). After each coupling, the fmoc protective group was cleaved off by a 25% piperidine solution in DMF (dimethyl-formamide) in an 11 minutes reaction step.

Peptides were sequentially synthesized, beginning at the C-terminus. The N-terminal proline was introduced as t-Boc-proline.

For introduction of DOTA (1,4,7,10-tetraacacyclododecane), the Mmt protective group was cleaved off by repeated treatment with a solution of 1% TFA (trifluor acetic acid) and 1% TIPS (triisopropylsilane) in DCM during one hour. After several washing steps with DMF and neutralising of the resulting TFA-salt with DIPEA the deprotected side chain was accessible for DOTA coupling. Coupling was carried out with 3 equivalents of 1,4,7,10-tetraacacyclododecane-1,4,7-tris(tert.butylester)-10-acetic acid (Macrocyclics, Dallas, USA), 3 equivalents of TBTU and 6 equivalents of DIPEA during 1,5 hours at room temperature. Then the Dde side chain protective group was cleaved off by repeatedly treating the resin with a solution of 2.5% hydrazinhydrate in DMF over the course of one hour. After several washing steps with DMF, the fluorescein urea derivate was coupled to the peptide using 0.5 mM fluorescein-5-isothiocyanate with equal amount of DIPEA in DMSO (dimethylsulfoxide) at room temperature over night. The peptide resin was then washed with DMF, methanol and DCM.

Cleavage of the remaining side chain protective groups was carried out simultaneously with cleavage of the peptide from the resin in one final step. The dry resin was therefore stirred at room temperature for 3 hours in a mixture of 12 ml TFA, 0.3 ml ethandithiol (EDT), 0.3 ml anisole, 0.3 ml water and 0.1 ml TIPS.

The peptide was then precipitated with cold pure diethyl ether, filtered, washed again with ether and dried in vacuum. The resulting raw peptide was purified *via* semipreparative HPLC (high performance liquid chromatography). Equimolar amounts of Gd-chloride solution were applied to the DOTA-peptides, pH was set to 5.2-5.6 using 0.1M NaOH and the mixture was stirred at 50 °C for 5 hours. After neutralisation with a few drops of acetic acid, the solution was lyophilised. The resulting Gd-containing and Gd-free DOTA-conjugates were shown to be ≥ 97% pure by analytical HPLC, and their molecular weights were determined by electrospray ionization mass spectrometry (ESI-MS).

2.2. Electrospray Ionization Mass Spectrometry (ESI-MS)

The conjugates (Table (**1**)) were analyzed by ESI-MS on an Esquire3000+ ion trap mass spectrometer (Bruker-Daltonics, Bremen, Germany). They were dissolved in 40% ACN, 0.1% formic acid in water (v/v/v) (20 pmol/µl) and constantly infused using a syringe pump (5 µl/min flow rate). Mass spectra were acquired in the positive ion mode (Fig. **1**). Dry gas (6 l/min) temperature was set to 325 °C, the nebulizer to 20.0 psi, and the electrospray voltage to -3700 V.

Table 1. Conjugates NLS, HIV-NLS, AHX-NLS and Gd-NLS, Gd-HIV-NLS, Gd-AHX-NLS

NLS	**PKKKRKVK(FITC)GGK(DOTA)**
HIV-NLS	**PKKKRKVRKKRRQRRRK(FITC)GGK(DOTA)**
AHX-NLS	**PKKKRKVRXRXRXRXRXRXRK(FITC)GGK(DOTA)**
Gd-NLS	**PKKKRKVK(FITC)GGK(GdDOTA)**
Gd-HIV-NLS	**PKKKRKVRKKRRQRRRK(FITC)GGK(GdDOTA)**
Gd-AHX-NLS	**PKKKRKVRXRXRXRXRXRXRK(FITC)GGK(GdDOTA)**

Conjugates NLS, HIV-NLS, AHX-NLS and Gd-NLS, Gd-HIV-NLS, Gd-AHX-NLS.

Single-Letter Amino Acid Code: K, lysine; R, arginine; P, proline; V, valine; Q, asparagine.

X, aminohexanoic acid.

DOTA, 1,4,7,10- tetraazacyclododecane-1,4,7,10-tetraacetic acid.

Gd, gadolinium.

FITC, fluorescein isothiocyanate.

NLS

calculated mass (m/z):
2028.08 $[M+H]^+$ (monoisotopic)
measured mass (m/z):
2028.07 $[M+H]^+$(monoisotopic)

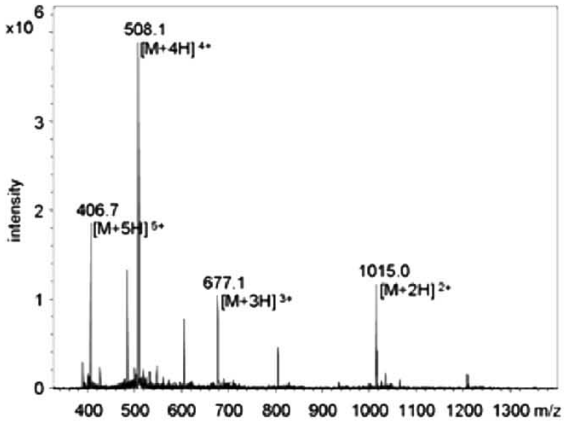

Gd-NLS

calculated mass (m/z):
2182.99 $[M+H]^+$ (monoisotopic)
measured mass (m/z):
2183.14 $[M+H]^+$(monoisotopic)

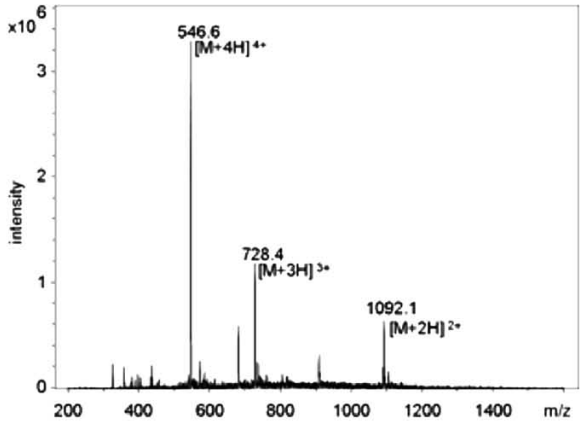

HIV-NLS

calculated mass (m/z):
3348.94 $[M+H]^+$ (monoisotopic)
measured mass (m/z):
3348.90 $[M+H]^+$(monoisotopic)

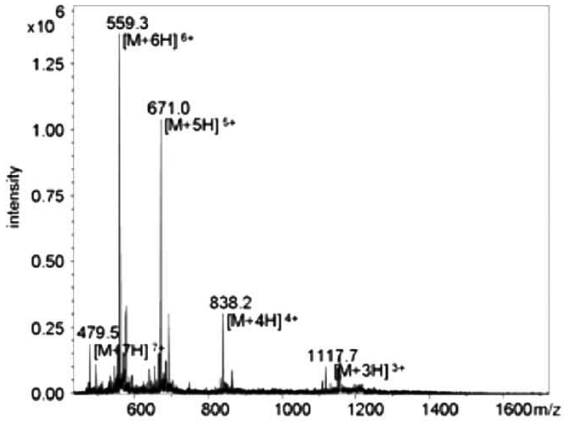

Gd-HIV-NLS

calculated mass (m/z):
3503.84 $[M+H]^+$ (monoisotopic)
measured mass (m/z):
3503.92 $[M+H]^+$(monoisotopic)

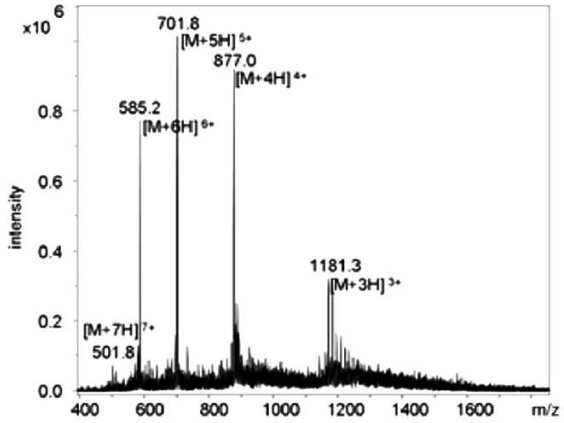

AHX-NLS

calculated mass (m/z):
3799.30 $[M+H]^+$ (monoisotopic)
measured mass (m/z):
3799.35 $[M+H]^+$(monoisotopic)

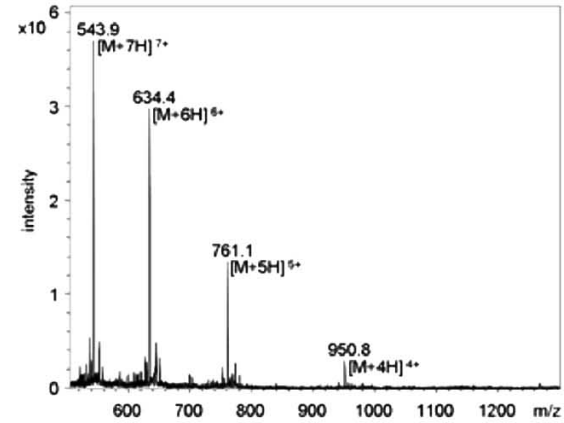

Gd-AHX-NLS

calculated mass (m/z):
3954.20 $[M+H]^+$ (monoisotopic)
measured mass (m/z):
3954.19 $[M+H]^+$(monoisotopic)

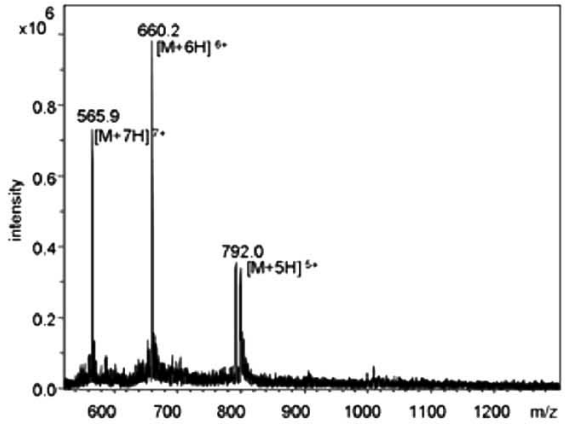

Fig. (1). ESI mass spectra (positive ion mode, gadolinium free and gadolinium containing conjugates).

2.3. Confocal Laser Scanning Microscopy (CLSM)

All cells were grown to 80% confluency in 75 cm^2 culture flasks (Corning Costar, Bodenheim, Germany) at 37°C in an atmosphere of 5% CO_2 (v/v).

Accutase™ (PAA laboratories, Pasching, Austria) was added to detach the cells which were harvested and subsequently transferred to 16-well plates (NUNC, Wiesbaden, Germany) [37°C, 5% CO_2 (v/v)]. Cells (80% confluency) were incubated with Dulbecco´s phosphate buffered saline (D-PBS; GIBCO; Invitrogen, Germany) alone (negative controls) and with 260 µM solutions of the conjugates in D-PBS for 20 minutes. After this, the cells were rinsed three times with buffer and then incubated with RPMI 1640 Ready Mix Medium (PAA laboratories) again.

PI was added to the medium (1-5 µmol l^{-1} PI; Molecular Probes, Eugene, OR, USA) to detect cells with damaged cell membranes.

The FITC-labelled conjugates were detected by confocal laser scanning microscopy. Confocal laser scanning microscopy was performed on an inverted LSM 510 laser scanning microscope (Carl Zeiss, Jena, Germany) (objectives: LD Achroplan 40 x 0.6, Plan Neofluar 20x0.50, 40x0.75). For fluorescence excitation, the 488 nm line of an argon laser and the 543 nm line of a HeNe laser with appropriate beam splitters and barrier filters were used for FITC and PI, respectively. Superimposed images of FITC- and PI-stained samples were created by overlaying coincident views. All measurements were performed at least three times in living cells.

2.4. Evaluation of Confocal Laser Scanning Using the Image J Software

Images of adherent cells were acquired (see confocal laser scanning) and converted to jpg format with the LSM Image Browser software (Zeiss, Germany). Using the Image J software the mean brightness values of stained and non-stained cells (~150 cells per incubation), as well as the mean brightness of the background were acquired and listed. The threshold for cell staining was observed at a brightness value equal to the background value +10%. Three independent incubations were evaluated and the results were listed.

PI staining was evaluated using pictures showing the fusion of the PI channel and the transmission channel. All PI-stained and non-stained cells in a picture sector (~300 cells) were counted and the staining ratio was determined. This was performed for pictures of 3 independent incubations. Mean staining ratio and deviation are presented (Fig. (**3a**)).

2.5. Magnetic Resonance (MR) Relaxometry

For MR relaxometry, human U373 and LN 18 glioma cells were grown in 75 cm^2 culture flasks (Corning Costar, Bodenheim Germany) (70% confluency). Accutase™ (PAA laboratories, Pasching, Austria) was added to achieve detachment of the cells, which were harvested and subsequently aliquoted into Eppendorf tubes (6 x 10^6 cells per tube). As in the investigations performed by fluorescence microscopy, the cells in the first tube served as a control (PBS only). The cells in the other tubes were incubated with conjugates **Gd-NLS**, **Gd-HIV-NLS** and **Gd-AHX-NLS** (260 µM). After a twenty-minute incubation period at 37°C in an atmosphere of 5% CO_2, the cells were washed three times in PBS and centrifuged at 800 rpm for 5 min.

In vitro imaging was performed with a 3 Tesla whole body MRI-system (Trio, Siemens Magnetom Sonata, circular polarised extremity coil, Siemens, Erlangen, Germany).

Sagittal T1-weighted MR images were obtained using the following spin echo sequence:

TR (repetition time): 200 ms, TE (echo time): 7.4 ms, flip angle 90°, averages: 1, concatenations: 2, measurements: 1, number of slices: 19, distance factor: 30%, slice thickness: 3 mm, field of view read: 180 mm, field of view phase: 100%, base resolution: 256, phase resolution: 100%, voxel size: 0.7 x 0.7 x 3.0 mm, scan time: 1:48 min.

T1 relaxation times were evaluated from signal intensities obtained by multiple axial spin echo measurements:

TR: 20-8000 ms (50 different TR values), TE: 6.4 ms, flip angle 90°, averages: 1, measurements: 1, number of slices: 1, slice thickness: 1 mm, field of view read: 120 mm, field of view phase: 87.5, base resolution 128, phase resolution: 100%, voxel size: 0.9 x 0.9 x 1 mm.

Analyses and calculations were performed using a Matlab program (Math Works, Natick, MA, USA). T1 values were estimated by a two-parameter fit procedure.

All signal curves were examined and found to be monoexponential.

The investigations were performed in five times.

2.6. Flow Cytometry

Fluorescence activated cell sorting (FACS) was performed using a Becton Dickinson FACSCalibur. 1 x 10^6 cells were incubated in 100 µl of conjugate solutions (260 µM in PBS) or PBS alone for 20 minutes. Then 300 µl FACS buffer (D-PBS containing 1% paraformaldehyde) was added. The samples were measured immediately. Approximately 25.000 events were recorded per sample. Fluorescence excitation was achieved by an Argon laser (488 nm). Fluorescence was detected using a 540-565 nm bandpass filter.

For FACS evaluation the mean FITC fluorescence intensity for each conjugate was acquired using the WinMDI software (Joseph Trotter, Scripps Research Institue, San Diego, CA, USA). All investigations were performed in triplicate and statistically evaluated.

3. RESULTS

3.1. Synthesis of Conjugates

FITC-labelled gadolinium-free and gadolinium-containing DOTA conjugates were synthesized (Table (**1**)). Molecular masses were determined by electrospray ionisation mass spectrometry [(**NLS**: calculated mass: 2028.08 Da, measured mass: 2028.07 Da); (**Gd-NLS**: calculated mass: 2182.99 Da, measured mass: 2183.14 Da); (**HIV-NLS**: calculated mass: 3348.94 Da, measured mass 3348.90 Da);

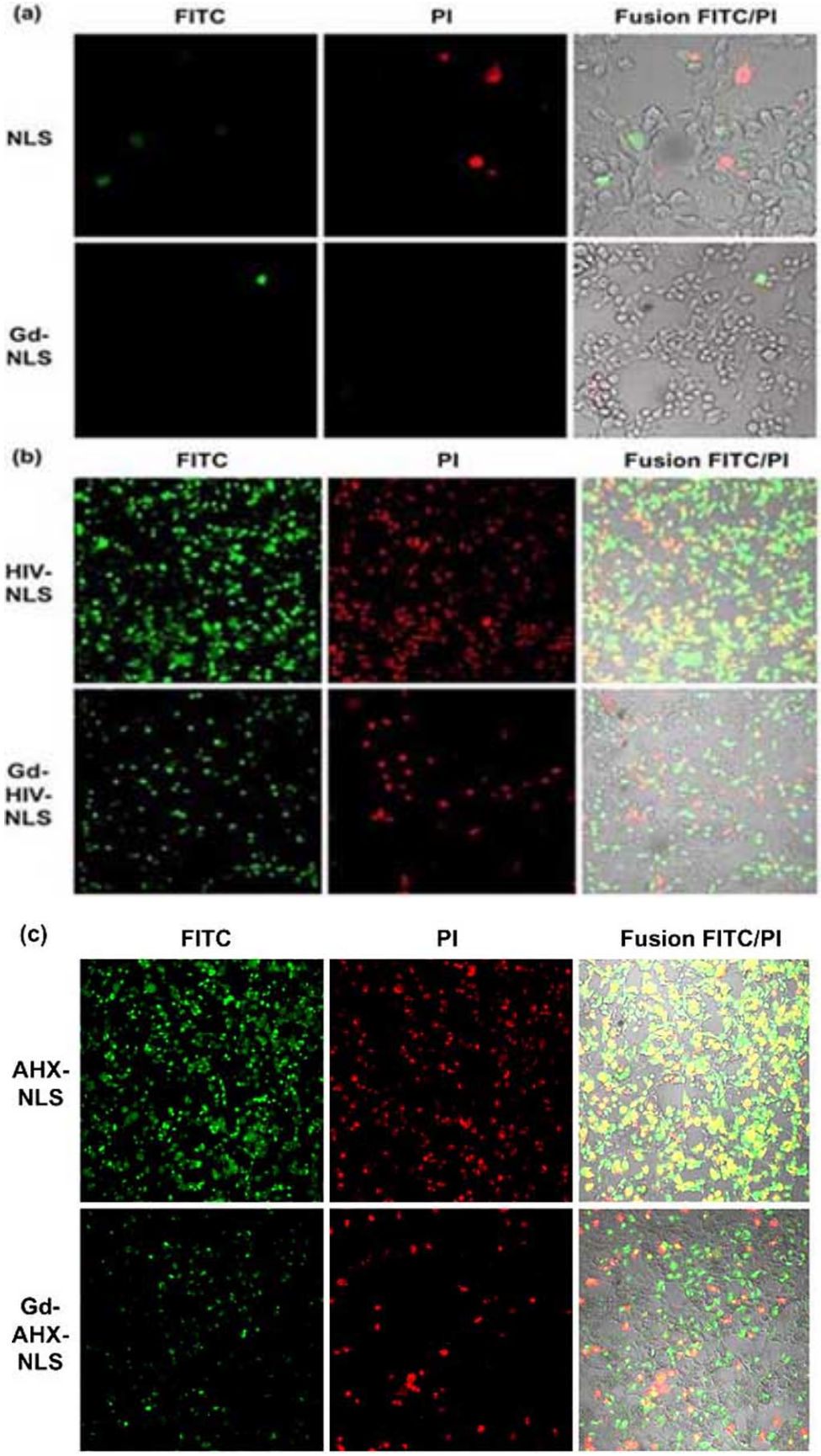
(a)
FITC
PI
Fusion FITC/PI
NLS
Gd-NLS
(b)
FITC
PI
Fusion FITC/PI
HIV-NLS
Gd-HIV-NLS
(c)
FITC
PI
Fusion FITC/PI
AHX-NLS
Gd-AHX-NLS

(Fig. 2. Contd….)

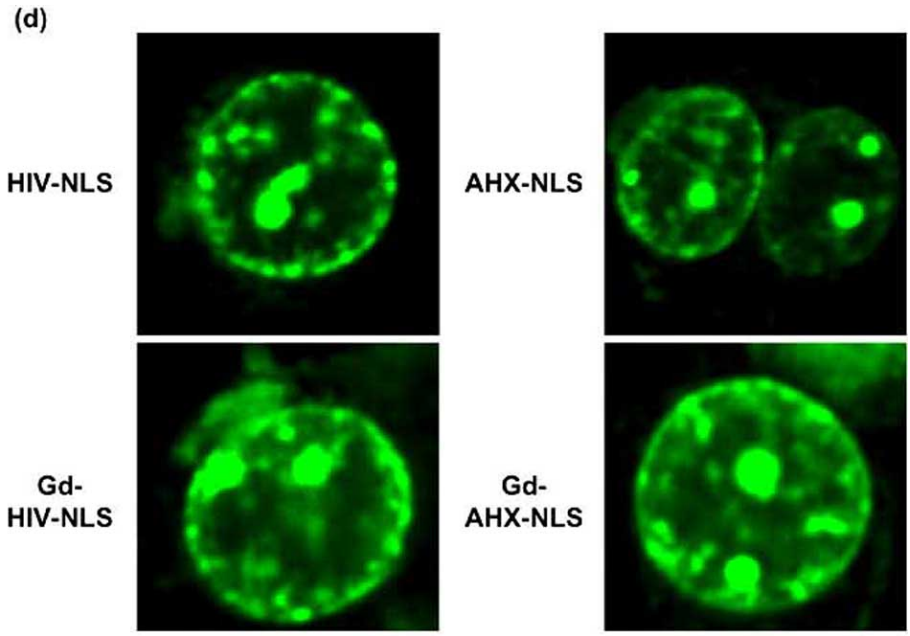

Fig. (2). CLSM images of human malignant U373 glioma cells.

a) No signs of cell death [no uptake of propidium iodide (PI)] and only a weak staining rate were observed after incubation with the gadolinium containing conjugate **Gd-NLS** and the non-gadolinium-containing conjugate **NLS**. Slightly more cells were stained with the non-gadolinium-containing conjugate **NLS**.

b) Much more cells were stained after incubation with conjugate **HIV-NLS**. Most of these cells showed signs of cell death (uptake of PI, red). Conjugate **Gd-HIV-NLS** stained a smaller fraction of cells, with most of them remaining viable (no uptake of PI).

c) Compared to conjugate **HIV-NLS** the number of stained cells could be further increased by using conjugate **AHX-NLS**. The stained cells were dead (uptake of PI). By contrast fewer cells were stained by conjugate **Gd-AHX-NLS**. Many of the stained cells remained viable (no uptake of PI).

d) Close-up images after incubation with conjugates **HIV-NLS**, **Gd-HIV-NLS**, **AHX-NLS** and **Gd-AHX-NLS** show the nuclear localization of the conjugates. (For interpretation of the references to colour in this figure, the reader is referred to the web version of this paper)

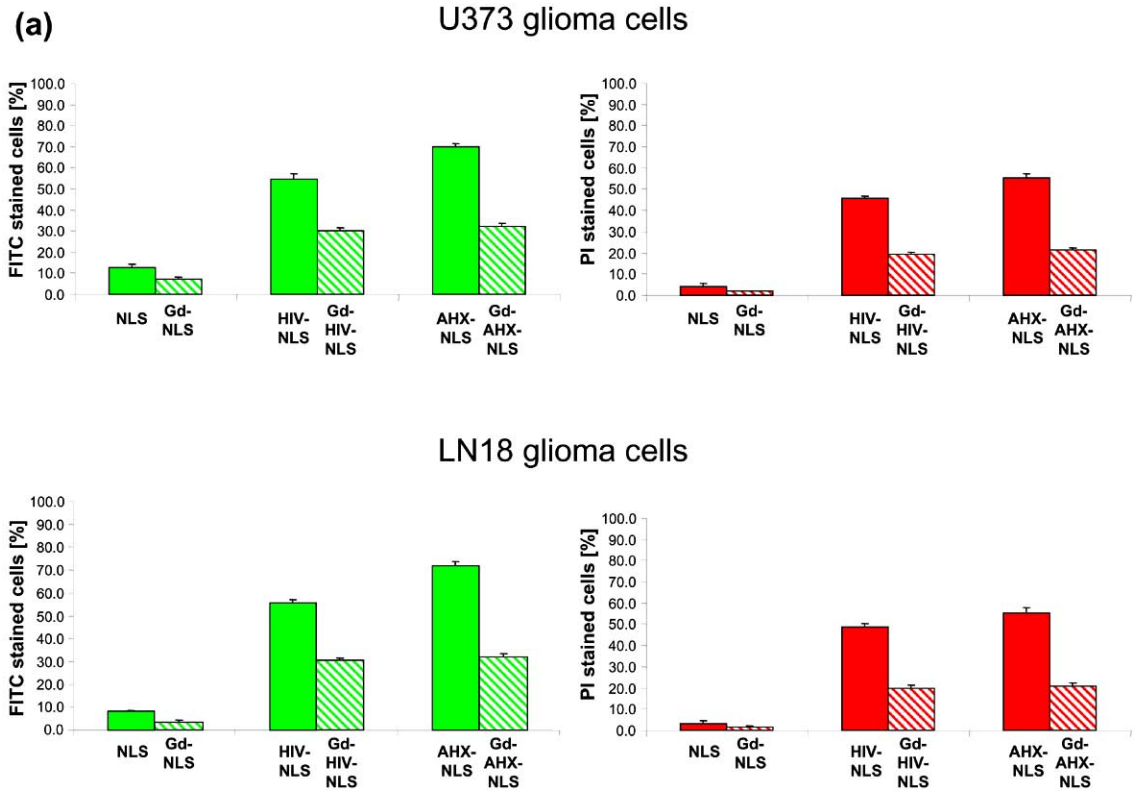

(Fig. 3. Contd….)

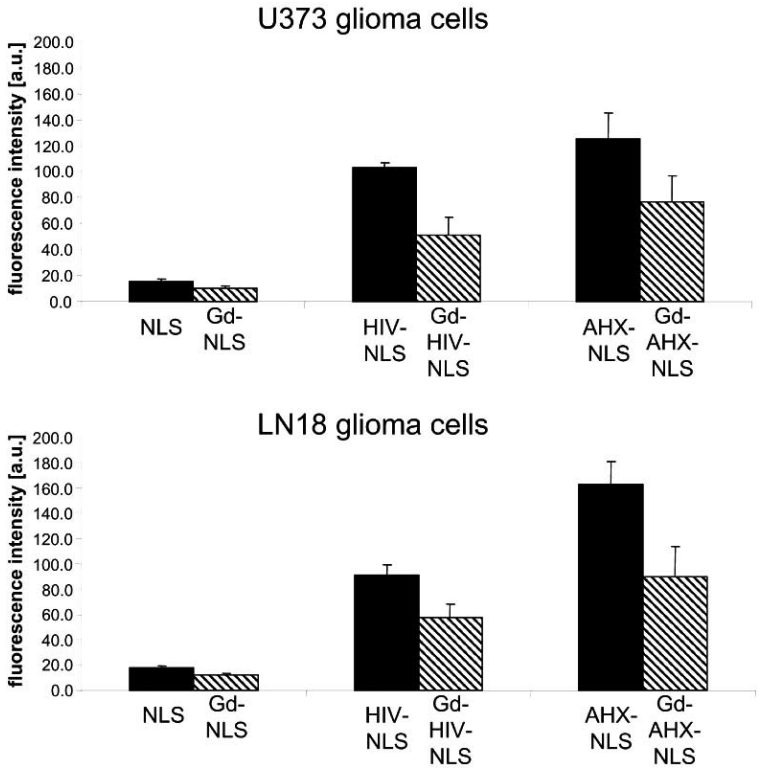

Fig. (3).

a) Percentage of FITC- and PI-stained cells after incubation with the Gd-free conjugates and the Gd-containing conjugates.

Compared to the conjugate **NLS** (FITC: 8-12%, PI: 3-4%), conjugate **HIV-NLS** (FITC: 52-57%, PI: 45-50%) showed a clearly higher number of FITC- and PI-stained cells. Conjugate **AHX-NLS** (FITC: 68-73%, PI: 54-58%) presented with even stronger FITC- and PI-staining.

Conjugate **Gd-NLS** (FITC: 4-8%, PI: 1-2%) showed weaker staining than conjugate **NLS**. Incubation with conjugates **Gd-HIV-NLS** (FITC: 29-32%, PI: 19-22%) and **Gd-AHX-NLS** (FITC: 31-34%, PI: 20-22%) led to comparable FITC- and PI-staining, which was stronger than for conjugate **NLS**, but much weaker than for conjugates **HIV-NLS** and **AHX-NLS**.

The examinations were performed three times. The standard deviation of the mean is depicted.

b) FACS (fluorescence activated cell sorting) analysis showed low mean fluorescence intensity after incubation with conjugate **NLS**.

Incubation with conjugate **HIV-NLS** resulted in 4-5fold increase in mean fluorescence intensity compared to conjugate **NLS**, while incubation with conjugate **AHX-NLS** led to a 6-8fold increase in mean fluorescence intensity compared to **NLS**.

Although the absolute mean fluorescence intensity values were lower for the gadolinium-containing conjugates, they showed the same mean fluorescence intensity distribution as their gadolinium-free counterparts.

The FACS analysis was performed in triplicate. Mean values and standard deviation are displayed. (For interpretation of the references to colour in this figure, the reader is referred to the web version of this paper)

(**Gd-HIV-NLS**: calculated mass: 3503.84 Da, measured mass: 3503.92 Da); (**AHX-NLS**: calculated mass 3799.30 Da, measured mass 3799.35 Da); (**Gd-AHX-NLS**: calculated mass: 3954.20 Da, measured mass: 3954.19 Da)] (Fig. (**1**)).

3.2. Confocal Laser Scanning Microscopy, Viability Tests and Flow Cytometry

The conjugates were evaluated by confocal laser scanning microscopy.

The conjugate **NLS** resulted in weak staining with regard to the number of positive cells (8-12%, Figs. (**2a**), (**3a**) and staining intensity (Fig. (**3a**)) in the cytoplasm and nucleus. Only minimal propidium iodide (PI) uptake (marker for disrupted cell membranes) was observed.

By contrast, the application of conjugate **HIV-NLS** resulted in strong cytoplasmic and nuclear staining with a much higher percentage of positive cells (54-57%, Figs. (**2b**), (**3a**)) which was further increased after incubation with conjugate **AHX-NLS** (68-73%, Figs. (**2c**), (**3a**)).

A high percentage of cells stained by **HIV-NLS** and **AHX-NLS** were nonviable, as shown by the nuclear uptake of PI (Figs. (**2b**), (**c**), (**3a**)).

The cellular and nuclear uptake ratio of the gadolinium-containing DOTA conjugates (**Gd-NLS**, **Gd-HIV-NLS**, **Gd-AHX-NLS**) was diminished to about half of that of their gadolinium-free counterparts (Figs. (**2a-c**), (**3**)).

For conjugates **HIV-NLS**, **AHX-NLS**, **Gd-HIV-NLS** and **Gd-AHX-NLS** there appears to be a constant relation between FITC- and PI-staining.

3.3. Magnetic Resonance Relaxometry

No marked shortening of T1 relaxation times compared to those obtained from the native control was observed after incubation with conjugate **Gd-NLS** (130 μM) (Fig. (**4**)).

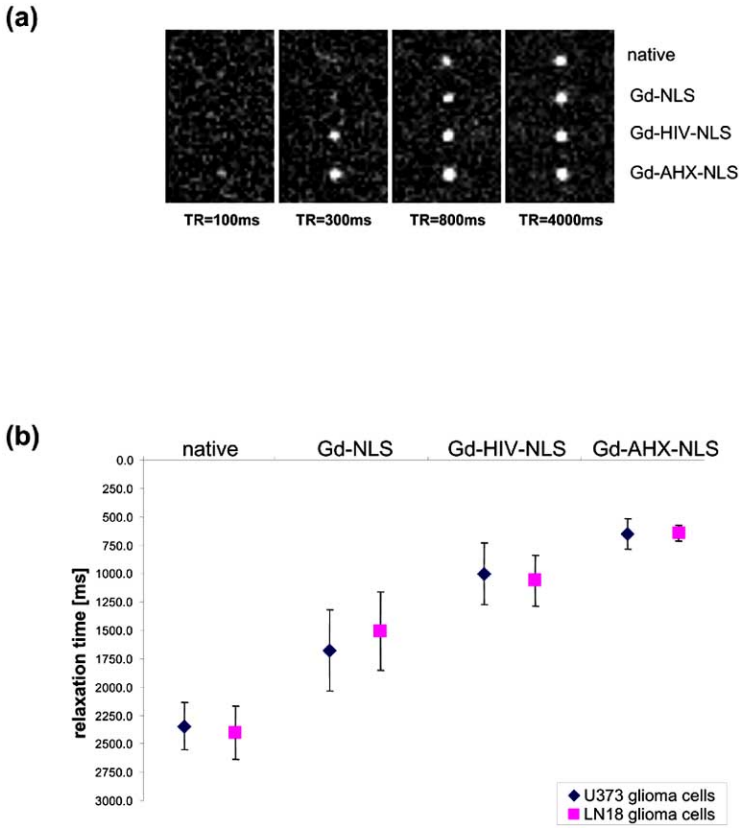

Fig. (4).

a) MR relaxometry of U373 glioma cells (about 6 x 10^6 cells per sample).

T1-images with different TR-values are exemplarily shown (TR=100, TR=300, TR=800, TR=4000).

After incubation with conjugate **Gd-AHX-NLS** U373-glioma cells show an increase of signal intensity already at TR: 100 ms.

Conjugate **Gd-HIV-NLS** was the second strongest contrast agent, followed by conjugate **Gd-NLS** and the native control.

b) T1 relaxation times of U373 (blue) and LN18 (pink) glioma cells after incubation with PBS alone and conjugates **Gd-NLS**, **Gd-HIV-NLS** and **Gd-AHX-NLS**.

The y-axis is inverted to reflect the fact, that the lowest T1 relaxation times indicate the strongest contrast agents.

The native control shows the longest T1 relaxation time (lowest intensity), followed by conjugate **Gd-NLS**. T1 relaxation time for conjugates **Gd-HIV-NLS** and **Gd-AHX-NLS** are even shorter, with conjugate **Gd-AHX-NLS** showing the shortest relaxation time at about 650 ms for both glioma cell lines.

The examinations were performed five times. The standard deviation from the mean is depicted. (For interpretation of the references to colour in this figure legend, the reader is referred to the web version of this paper)

However, there was a distinct shortening of T1-relaxation times after incubation with the conjugate **Gd-HIV-NLS**, and these decreased further after incubation with conjugate **Gd-AHX-NLS** (Fig. (**4**)).

4. DISCUSSION

DOTA-SV 40 T antigen NLS conjugates elongated by four arginines were found to be taken up by no more than 35% of U373 and LN18 glioma cells.

With the aim to ameliorate the cellular uptake rate, we produced DOTA-SV 40 T antigen NLS conjugates in which the four arginines were replaced by the basic domain $Tat_{49–57}$ of HIV-1 (**HIV-NLS**) or a novel peptide containing 7 arginines and 6 aminohexanoic acids (**AHX-NLS**). As a control we used the DOTA-SV 40 T antigen NLS conjugate without any cationic peptide sequence (**NLS**) (Table (**1**)).

Conjugate **NLS** (Table (**1**)) was transported not only across the external cell membrane but also across the nuclear membrane but only in a small percentage of cells (10-12%, Figs. (**2a**), (**3a**)). A comparable low cellular uptake rate of an ^{111}In labelled DOTA-SV 40 T antigen NLS conjugate without FITC-label was previously described by Ginj *et al*., 2005 [8]. This is surprising because several other compounds (e.g. cobaltocenium and DNA intercalating pyrene) have been transported successfully across the cellular and nuclear membrane using the NLS of the SV 40 T antigen alone [9], [10].

Our conjugate **HIV-NLS** (Table (**1**)) was associated with a remarkable increase in nuclearly-stained cells as well as mean fluorescence intensity, which was shown by confocal laser scanning microscopy and fluorescence activated cell sorting (Figs. (**2b**), (**3**)). Even more cells were stained after

exchange of HIV1-tat within the conjugate HIV-NLS by the R7Ahx6-peptide resulting in conjugate **AHX-NLS** (Figs. (**2c**), (**3**)). This increase in staining was also reflected in the MRI findings, with shorter T1 relaxation times for conjugates **Gd-HIV-NLS** and **Gd-AHX-NLS** compared to conjugate **Gd-NLS** (Fig. (**4b**)). It remains unclear why a large fraction of the cells remained unstained by conjugate **NLS**. The much greater number of cells stained by conjugates **HIV-NLS** and **AHX-NLS** in comparison to conjugate **NLS** could be explained by the presence of HIV1Tat_{49-57}- or R7Ahx6-peptide within the DOTA-NLS conjugates. Conjugates **HIV-NLS** and **AHX-NLS** might have a higher transmembrane transport capacity than conjugate **NLS** due to the larger number of cationic amino acids. However, even conjugates **HIV-NLS** and **AHX-NLS** failed to stain a considerable part of the cells at the concentration used in the study (260 μM) (Fig. (**2b**,**c**)), indicating that these cells react differently towards the conjugates. It is unclear whether the cellular uptake of the NLS-coupled conjugates depends on the cell cycle stage, as has been shown for nuclear uptake [11], or on some other kind of cell heterogeneity. The composition of the cell membrane probably changes according to the cell cycle stage or may even differ amongst the individual cells of a specific cell line. However, different glioma cell lines (U373 and LN18) were found to display the same uptake behavior.

The most surprising finding of our experiments was the difference in cell viability associated with the three conjugates. Whereas only minimal effect on cell viability was found for conjugate **NLS**, a high cell death rate was observed after incubation with conjugates **HIV-NLS** and **AHX-NLS**, as demonstrated by the uptake of propidium iodide.

The reason for this cell death is unclear. To exclude the possibility that it had resulted from the toxic effects of free gadolinium, the conjugates were produced with and without gadolinium.

The intracellular release of toxic free gadolinium from the complex cannot be excluded but seems to be less likely because the gadolinium-free DOTA conjugates **HIV-NLS** and **AHX-NLS** showed higher cellular uptake associated with a higher cytotoxic potential when compared with their gadolinium-containing counterparts. Furthermore the Gd-DOTA-complex is known to be very stable with a half-life of 4000 hours (pH2) [12,13]. It is known that the HIV-1 tat peptide may induce apoptosis in hippocampal cells [14].

Therefore, it seems possible that the combination of both the NLS of the SV 40 T antigen and the HIV-1 tat-peptide and DOTA in the conjugates might be the factor responsible for cell death. However, even stronger cytotoxic potential can be attributed to conjugate **AHX-NLS** containing the novel R7Ahx6- instead of HIV-1 Tat_{49-57}-peptide. Additionally no cell death was reported after incubation of cells with the Gd-DOTA-complex only coupled to HIV1Tat_{49-57}-peptide [15,16].

Statistical evaluation revealed that cytotoxicity correlates strongly with the degree of cellular uptake independent of conjugate type.

The coupling of NLSs to the Gd-DOTA complex does not automatically lead to nuclear accumulation, as has been shown by Allen and Meade [17]. They synthesized a gadolinium conjugate of comparable size to conjugates **Gd-HIV-NLS** and **Gd-AHX-NLS** (Gd-DOTA-complex bound to 16 arginine also harboring NLSs e.g. RRRRRR: NLS of p85s6k [18]). Their conjugate was also taken up by the cytoplasm but did not permeate the cell nucleus, although nuclear staining resulting from passive diffusion might be expected in the case of molecules of less than 10 kDa [19].

We evaluated magnetic resonance relaxivity from the single measurements obtained for varying repetition time (TR) values (Fig. (**4a**)). These measurements allow the concentration of the Gd-DOTA complex in the cell pellets to be determined, which is not possible from signal intensity values obtained for a single TR value. By obtaining a large number of measurements for varying TR values it is possible to determine whether the relaxation curves are monoexponential (one component) or biexponential (two components). All the relaxation curves recorded were found to be monoexponential, so that this method was not able to detect the presence of two classes of cells (i.e., stained and non-stained). However, a close correlation between relaxivity and the concentration of the Gd-DOTA complex in the whole cell pellet was found (Fig. (**4b**)).

In summary, a higher cellular and nuclear uptake rate of an FITC-labelled DOTA-SV 40 T antigen NLS conjugate could be achieved by elongation with either the HIV-1 Tat_{49-57}-peptide or the novel R7Ahx6-peptide. This was associated with a high cell death rate.

The cytotoxic properties exhibited by these conjugates correlate with the cellular uptake and thus with the MRI signal intensity. Therefore such conjugates could find application in intraoperative tumor imaging combined with chemotherapy.

The presence of gadolinium within the FITC-labelled DOTA conjugates was associated with a reduced cellular uptake. This might result from the loss of DOTA's carboxyl-groups after complexation of DOTA with gadolinium and was already observed with smaller DOTA conjugates [4].

ACKNOWLEDGEMENT

The study was supported by the Hertie-Foundation for Brain Research.

REFERENCES

[1] Corot, C.; Port, M.; Raynal, I.; Dencausse, A.; Schaefer, M.; Rousseaux, O.; Simonot, C.; Devoldere, L.; Lin, J.; Foulon, M.; Bourrinet, P.; Bonnemain, B.; Meyer, D. Physical, Chemical, and biological evaluations of P760: a new gadolinium complex characterized by a low rate of interstitial diffusion. *J. Magn. Reson. Imaging,* **2000**, *11*,182-91.

[2] Le Mignon, M.M.; Chambon, C.; Warrington, S.; Davies, R.; Bonnemain, B. Gd-DOTA. Pharmacokinetics and tolerability after intravenous injection into healthy volunteers. *Invest. Radiol.,* **1990**, *25*, 933-7.

[3] Kalderon, D.; Roberts, B.L.; Richardson, W.D.; Smith, A.E. A short amino acid sequence able to specify nuclear location. *Cell,* **1984**, *39*, 499-509.

[4] Sturzu, A.; Regenbogen, M.; Klose, U.; Echner, H.; Gharabaghi, A.; Heckl, S. Novel dual labelled nucleus-directed conjugates containing correct and mutant nuclear localisation sequences. *Eur. J. Pharm. Sci.,* **2008**, *33*, 207-16.

[5] Vives, E.; Brodin, P.; Lebleu, B. A truncated HIV-1 Tat protein basic domain rapidly translocates through the plasma membrane and accumulates in the cell nucleus. *J. Biol. Chem.,* **1997**, *272*, 16010-7.

[6] Wender, P.A.; Mitchell, D.J.; Pattabiraman, K.; Pelkey, E.T.; Steinman, L.; Rothbard, J.B. The design, synthesis, and evaluation of molecules that enable or enhance cellular uptake: peptoid molecular transporters. *Proc. Natl. Acad. Sci. USA,* **2000**, *97*, 13003-8.

[7] Minnicozzi, M.; Ramirez, M.M.; Egan, R.W.; Gleich, G.J.; Kobayashi, I.; Kim, D.; Duran, W.N. Polyarginine and eosinophil-derived major basic protein increase microvascular permeability independently of histamine or nitric oxide release. *Microvasc. Res.,* **1995**, *50*, 56-70.

[8] Ginj, M.; Hinni, K.; Tschumi, S.; Schulz, S.; Maecke; H.R. Trifunctional Somatostatin-Based Derivatives Designed for Targeted Radiotherapy Using Auger Electron Emitters. *J. Nucl. Med.,* **2005**, *12*, 2097-103.

[9] Noor, F.; Wüstholz, A.; Kinscherf, R.; Metzler-Nolte, N.A. Cobaltocenium-Peptide Bioconjugate Shows Enhanced Cellular Uptake and Directed Nuclear Delivery. *Angew. Chem. Int. Ed.,* **2005**, *44*, 2429-32.

[10] Haefliger, P.; Agorastos, N.; Renard, A.; Giambonini-Brugnoli, G.; Marty, C.; Alberto R. Cell Uptake and Radiotoxicity Studies of an Nuclear Localization Signal Peptide-Intercalator Conjugate Labeled with $[^{99m}Tc(CO)_3]^+$. *Bioconjug. Chem.,* **2005**, *16*, 582-7.

[11] Feldherr, C.M.; Akin, D. The permeability of the nuclear envelope in dividing and nondividing cell cultures. *J. Cell Biol.,* **1990**, 111, 1-8.

[12] Lukes, I.; Kotek, J.; Vojtisek, P.; Hermann, P. Complexes of tetraazacycles bearing methylphosphinic/phosphonic acid pendant arms with copper(II), zinc(II) and lanthanides (III). A comparison with their acetic acid analogues. *Coord. Chem. Rev.,* **2001**, *216*, 287-312.

[13] Magerstadt, M.; Gansow, O.A.; Brechbiel, M.W.; Colcher, D.; Baltzer, L.; Knop, R.H.; Girton, M.E.; Naegele, M. Gd(DOTA): an alternative to Gd(DTPA) as a T1,2 relaxation agent for NMR imaging or spectroscopy. *Magn. Reson. Med.,* **1986**, *3*, 808-12.

[14] Kruman, I.I.; Nath, A.; Mattson, M.P. HIV-1 protein Tat induces apoptosis of hippocampal neurons by a mechanism involving caspase activation, calcium overload, and oxidative stress. *Exp. Neurol.,* **1998**, *154*, 276-88.

[15] Bhorade, R.; Weissleder, R.; Nakakoshi, T.; Moore, A.; Tung, C.-H. Macrocyclic Chelators with Paramagnetic Cations Are Internalized into Mammalian Cells *via* a HIV-Tat Derived Membrane Translocation Peptide. *Bioconjug. Chem.,* **2000**, *11*, 301-5.

[16] Prantner, A.M.; Sharma, V.; Garbow, J.R.; Piwnica-Worms D. Synthesis and characterization of a Gd-DOTA-D-permeation peptide for magnetic resonance relaxation enhancement of intracellular targets. *Mol. Imaging,* **2003**, *2*, 333-41.

[17] Allen, M.J.; Meade, T.J. Synthesis and visualization of a membrane-permeable MRI contrast agent. *J. Biol. Inorg. Chem.,* **2003**, *8*, 746-50.

[18] Reinhard, C.; Fernandez, A.; Lamb, N.J.; Thomas, G. Nuclear localization of p85s6k: functional requirement for entry into S phase. *EMBO J.,* **1994**, *13*, 1557-65.

[19] Wei, X.; Henke, V.G.; Strübing, C.; Brown, E.B.; Clapham, D.E. Real-Time Imaging of Nuclear Permeation by EGFP in Single Intact Cells. *Biophys. J.,* **2003**, *84*, 1317-27.

Received: 28 August, 2008 Revised: 18 November, 2008 Accepted: 20 November, 2008